Národní konference s mezinárodní účastí

INŽENÝRSKÁ MECHANIKA 2002

13. – 16. 5. 2002, Svratka, Česká republika

Significance of the components non-linearities to the ride comfort optimization of a conceptual quarter-car model

Pavel Kvasnička, František Palčák

The main goal of this paper is to study how non-linearities of components and subjective ride comfort perception quantity assessment influence the ride comfort, and find the best setup of vehicle carrying spring and damper parameters via optimization of a conceptual quarter-car model.

In the paper is also a disscussion of how to create proper representative of the road exitation considering the properties of the stochastic road derived by power spectral density from time domain simulation.

Comparison of the results from numerical integration and from frequency domain analysis and the influence of simulation time and time step on frequency bandwidth and accuracy of the results are also mentioned.

Objective function for ride comfort optimization is in this paper defined as the sum of the normalized human perception quantity and the normalized normal tire force distribution.

Key words: car ride comfort, stochastic road, non-linearities of components

1 Introduction

Steady growing customers requirements for comfort and safe ride of personal cars force the automotive industry to stronger use of virtual prototyping of the cars including also the prediction of the ride comfort.

In the past, several empiric methods for describing the subjective human perception of the comfort were developed. Most of these can be characterised as filters of the excitation at relevant comfort points (for example the seat, steering wheel or the floor). Some of these methods were used in simple linear models (3-12 Dof) studying main influencies of the model parameters and of stochastic road excitation.

We will study the significance of the subjective human ride comfort perception for purpose of car optimization in the concept phase.

On the other hand, in the concept phase we face the problem of not knowing the car properties exactly, mainly the main non-linear vertical behavior (such as bumps, friction and non-linear damping). To answer the question of the significance of the non-linear behavior we have to look for the solution in the time domain.

Therefore the properties of a stochastic road and the possibilities of creating one representative from a power spectral density for a time domain simulation are discussed.

Further some of the perception quantity evaluation methods of ride comfort are cited and compared.

The results from numerical integration and from frequency domain analysis are evaluated to prove their acceptance. Also the influence of simulation time and time step on frequency bandwidth and accuracy of the results are studied.

Afterwards we can determine the influence of the components non-linearities to a possible optimization of a concept car model.

2 Stochastic road

If the car is driven on an uneven road under normal conditions (no hard braking, etc) we speak of the ride comfort. Supposed driving a straight line, every wheel is excited by stochastic unevenness. Many empirical tests have shown that the stochastic road excitation is an ergodic process. The one-sided power spectral density of a road can be represented by [1][2][3]:

$$G_{uu}(\Omega_x) = G_{uu}(\Omega_{x0})\left(\frac{\Omega_{x0}}{\Omega_x}\right)^w .$$

Where:

Ω_{x0} is the spatial angular reference frequency
$G_{uu}(\Omega_{x0})$ is the degree of roughness
w is the waviness

The Equation represents a straight line in a double logaritmic scale.

Usually w achieves values between 1.5 – 3, the parameter $G_{uu}(\Omega_{x0})$ between $0.3cm^{-3}$ and $62cm^{-3}$. For a federal road one can use 2 for the parameter w and 4 for the parameter $G_{uu}(\Omega_{x0})$.

For linear models we can use this equation as input using v as the driving velocity:

$$G_{uu}(\Omega) = \frac{G_{uu}(\Omega_{x0})}{v}\left(\frac{\Omega_{x0} v}{\Omega}\right)^w .$$

For non-linear models it is necessary to use a numeric simulation in the time domain. We can transform the excitation first to the spatial domain. Scanning the power spectral density we obtain the effective power value for a single frequency [11]:

$$\Delta h_{ieff}^2 = \frac{1}{2\pi} G_{uu}(\Omega_{xi}) * \Delta\Omega_x .$$

We can collect the whole signal: $h(x) = \sum_{i=1}^{N} C_i \sin\left((\Omega_{x\min} + (i-1)\Delta\Omega_x)x + \varphi_i\right),$

with: $C_i = \sqrt{\frac{1}{\pi} G_{uu}(\Omega_{xi}) * \Delta\Omega_x}$.

Since we generate only one represantative of the signal with the same power spectral density, the phase angle φ_i gets randomly distributed values between 0 and 2π.

There are still two variables $\Delta\Omega$ and the length of the generated road (size of the vector x) left, both are functions of the velocity. $\Delta\Omega$ is defined by the highest needed frequency in the result data. As we will see later, human comfort perception comprises frequencies up to 30Hz. Traveling with a velocity of 20m/s, $\Delta\Omega$ should be at least $0.6m^{-1}$, using Nyquist inequalence $0.166m^{-1}$. The length L of the vector x is also defined by the velocity and the Nyquist inequalence:

$L>(\omega_{min})^{-1}*v*(2.5 \text{ to } 4)$.

ω_{min} should be chosen small enough to not interfere with the system frequencies of interest. For example for $\omega_{min} = 0.1s^{-1}$ and velocity v=20m/s, L would be 500m to 800m.

3 Human perception of the vibration

The human response to vibration is dependent on the excitation frequency. The ISO 2631 uses a single DOF system to represent a human body [7]. VDI2057 presents curves of the constant perception for harmonic vibration [4][5][6]. Cucuz [8] developed numeric curves of perception and studied the influence of the stochastic and in-stationary vibration. He also introduced a correction factor C for the stochastic excitation. Klinger [9] gives explicit weightings for frequencies. Figure 1 shows the comparison of these methods. In practical use we understand these functions as filters of the human perception modulating the power spectral density of the e.g. seat acceleration. The standard deviation is then the perception quantity or K-value:

$$K_i = \sqrt{\int_0^\infty \phi_{Ki}(\Omega) d\Omega} \,.$$

Where for linear systems: $\Phi_{Ki} = C_i^2 B_i^2(\Omega) |H_i(\Omega)|^2 G_{uu}(\Omega)$,

with:

i	is the index for the measured postion (seat, hands, …)
C	is the factor for the stochastic excitation
B	is the frequency weighting function (the filter of the human perception)
H	is the transfer function from the tyre patch to the i position.
G_{uu}	is the power spectral density of the excitation

The resulting perception can be then calculated:

$$K^2 = \sum_i b_i^2 K_i^2 \,,$$

where b_i is the weighting factor for different position and direction to the perception quantity.

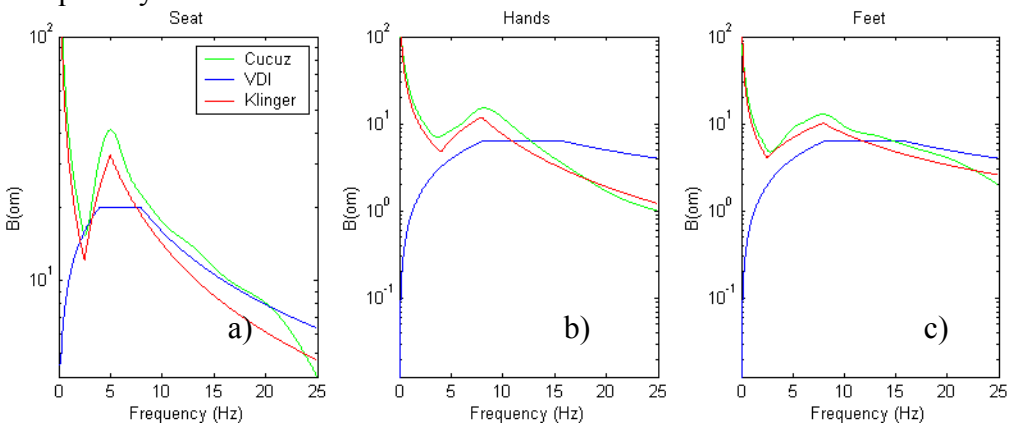

Figure 1: Seating human perception filters for **a)** seat **b)** hands and **c)** feet in logarithmic scale. Blue – VDI, Green – Cucuz, Red – Klinger

In Figure 1 a) one can note a high sensitivity of a seating human on vertical vibration at about 5Hz, same for all methods. Klinger and Cucuz filters behave nearly simillar in all perception criterias. One can markedly see a big difference between VDI and Cucuz/Klinger for low frequencies. This difference is less important because of the transfer functions from the road excitation to the seat,- hands,- or feet-acceleration , which are low for these frequencies.

4 Qurter car model

The quarter car can be used under the conditions developed in [10]:

- symetric vehicle about the length axis (no oscilation in x and y direction),

- same excitation for the left and right wheel (no roll angle oscilation),
- the motions of the for- and aftbody of the car are decoupled (long cars),
- driver is seating in the middle of the suspension (strong simplification for one driver),

it is possible to use a strongly simplified car model as pictured in Figure 2 a).

4.1 Linear quarter-car model

For $\underline{u}$:

$u_1 = z_s, u_2 = \dot{z}_s, u_3 = z_k, u_4 = \dot{z}_k, u_5 = z_r, u_6 = \dot{z}$.

Matrix notation in state space of such a linear model, also suitable for numeric integration is then:

$$\dot{\underline{u}} = A\underline{u} + Bh$$

$$\dot{\underline{u}} = \begin{bmatrix} 0 & 1 & 0 & 0 & 0 & 0 \\ -\frac{Cs}{Ms} & -\frac{Ds}{Ms} & \frac{Cs}{Ms} & \frac{Ds}{Ms} & 0 & 0 \\ 0 & 0 & 0 & 1 & 0 & 0 \\ \frac{Cs}{Mk} & \frac{Ds}{Mk} & -\frac{Ck+Cs}{Mk} & -\frac{Dk+Ds}{Mk} & \frac{Ck}{Mk} & \frac{Dk}{Mk} \\ 0 & 0 & 0 & 0 & 0 & 1 \\ 0 & 0 & \frac{Ck}{Mr} & \frac{Dk}{Mr} & -\frac{Ck+Cr}{Mr} & -\frac{Dk}{Mr} \end{bmatrix} \underline{u} + \begin{bmatrix} 0 \\ 0 \\ 0 \\ 0 \\ 0 \\ \frac{Cr}{Mr} \end{bmatrix} h \; .$$

4.2 Non-linear modificatios of the quarter-car model

The vertical dynamics of a personal car is in general non-linear. Stick-slip effects in the damper can occur. For larger vertical displacements of the carrying spring bump stops can progressively change its stiffness and fence the vertical motion. Vertical damping can be also non-linear. Considered all these effects, the linear quarter car model will be modified as shown in Figure 2 b).

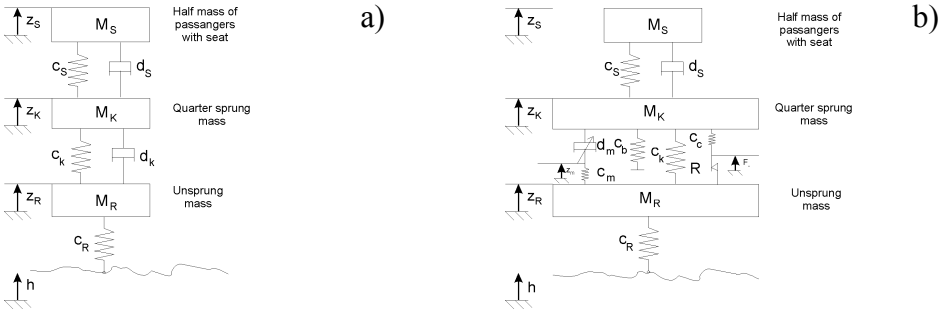

Figure 2: Quarter car dashpot model (3DOF) **a)** linear **b)** non-linear

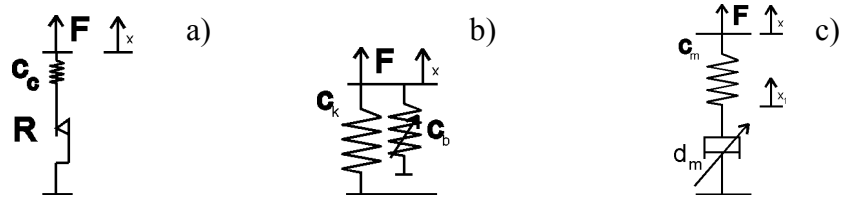

Figure 3: Rheologic Masing model of a **a)** Friction element. Scheme of **b)** a non-linear bump stop, **c)** a non-linear Maxwell element

- **Stick-Slip effects in the damper**

A car dashpot damper consists of sliding parts. Under non-axial forces acting on the damper (e.g. driving through a curve with the McPherson suspension) even a damper blocking can occur. From the ride comfort point of view small velocity amplitudes are important, because the viscous damping does not work yet. These effects can be described with the rheologic Masing element as shown in Figure 3 a).

Such an element can be described by the equation [12]:

$$\dot{F} = c_c \dot{x} \frac{1}{2}\left\{1 - \operatorname{sgn}\left(F^2 - R^2\right) - \operatorname{sgn}\left(\dot{x}F\right)\left[1 + \operatorname{sgn}\left(F^2 - R^2\right)\right]\right\}.$$

- **Bump stops**

Bump stops are additional springs on celasto material base. The stiffness function is progressive. Schematic picture is in Figure 3 b).

To describe the bump stop with parallel linear spring we will use the function:

$F = c_k x_0 + c_b (x - x_0)^3$.

The coefficients c_k and c_b can be identified by a polynomial fit of a displacement-force characteristic.

Because of saving development costs, very often the same bump stop is used for different springs. The change of the spring stiffness is then no more proportional to its linear part.

- **Non-linear damping**

It is advantageous to use a non-linear Maxwell element, which enables us also to take the bearing of a damper into account. A scheme is pictured in Figure 3 c).

Writing the force equilibrium: $c_m (x - x_1) = d_m (\dot{x}_1)$.

We get: $\dot{x}_2 = d_m{}^{(-1)}(k(x - x_1))$.

Where: $d_m(\dot{x}_2)$ is the force in the non-linear dashpot, calculated for example from a spline and c_m is the stiffness of the damper bearing

Hence we actually need the inverse function of the damper characteristic.

We can fit the inverse damper characteristic with a polynomial:

$d_m{}^{(-1)}(F) = aF^3 + bF^2 + cF + d$.

Both, the Masing and Maxwell elements introduce one new state variable each. For the Masing element the force itself is defined as a state variable. For the Maxwell element the internal displacement is a state variable. Both are represented by one differential equation of the first rang. During the integration we will use the half-implicit integration for the car system and an explicit integration for the Masing and Maxwell elements. The bump stop is defined directly and does no need any state equation. The non-linear car is then represented by the equations (see also Figure 2 b)):

$$\underline{\dot{u}} = A\underline{u} + Bh$$

$$\underline{\dot{u}} = \begin{bmatrix} 0 & 1 & 0 & 0 & 0 & 0 \\ -\frac{Cs}{Ms} & -\frac{Ds}{Ms} & \frac{Cs}{Ms} & \frac{Ds}{Ms} & 0 & 0 \\ 0 & 0 & 0 & 1 & 0 & 0 \\ \frac{Cs}{Mk} & \frac{Ds}{Mk} & -\frac{Ck+Cs}{Mk} & -\frac{Dk+Ds}{Mk} & \frac{Ck}{Mk} & \frac{Dk}{Mk} \\ 0 & 0 & 0 & 0 & 0 & 1 \\ 0 & 0 & \frac{Ck}{Mr} & \frac{Dk}{Mr} & -\frac{Ck+Cr}{Mr} & -\frac{Dk}{Mr} \end{bmatrix} \underline{u} + \begin{bmatrix} 0 \\ 0 \\ 0 \\ -\frac{F_{KR}}{Mk} \\ 0 \\ \frac{F_{KR}+Cr.h}{Mr} \end{bmatrix}$$

$$u_1 = z_s, u_2 = \dot{z}_s, u_3 = z_k, u_4 = \dot{z}_k, u_5 = z_r, u_6 = \dot{z}_r, u_7 = F_R, u_8 = z_m$$

$$\dot{u}_7 = c_c(\dot{u}_4 - \dot{u}_6)\frac{1}{2}\left\{1 - \operatorname{sgn}\left(u_7{}^2 - R^2\right) - \operatorname{sgn}((\dot{u}_4 - \dot{u}_6)u_7)\left[1 + \operatorname{sgn}\left(u_7{}^2 - R^2\right)\right]\right\}$$

$$\dot{u}_8 = d_m^{-1}(c_m(u_5 - u_8))$$

$$F_{KR} = u_7 + c_m(u_5 - u_8) + c_b(u_5 - u_3)$$

4.3 Numeric integration of the quarter car

For a linear model as introduced before, it is certainly possible to solve the perception quantity K using the frequency domain analysis (Chapter 3). We want study the non-linear modifications of the linear model. For this reason we will solve also the linear model using numerical integration in order to compare the obtained results with the results from frequency domain analysis.

Several methods can be used for the numeric integration. The Half-Implicit integration can be chosen as the most feasible method. It provides energy neutral behavior with larger possible integration step size. Small numerical damping in the system is important for perception quantity prediction.

Using numerical integration, the simulation time and the time step are important for the stochastic excitation. The time step has direct influence to the frequency bandwidth of the results. The simulated time has an influence on the accuracy of the results, since we study statistical values such as power spectral density.

First, in Figure 4 a) one can see the significance of the integration stepsize on the resulting power spectral density of the acceleration on the seat. The difference at higher frequencies is less important because of the filter functions of perception quantity, which strongly decease at higher frequencies. In Figure 4 b) the influence of the simulated time in terms of the traveled length for different stiffnesses of the carrying spring C_k is plotted. The difference in the power spectral density is important. The first peak of the 100m distance is 50% of the one with 900m. One can see that for the traveled distance of 100m the first peek is not clear enough (See also Figure 4 b), scaled part). Reason for this behaviour is explained in (Chapter 2).

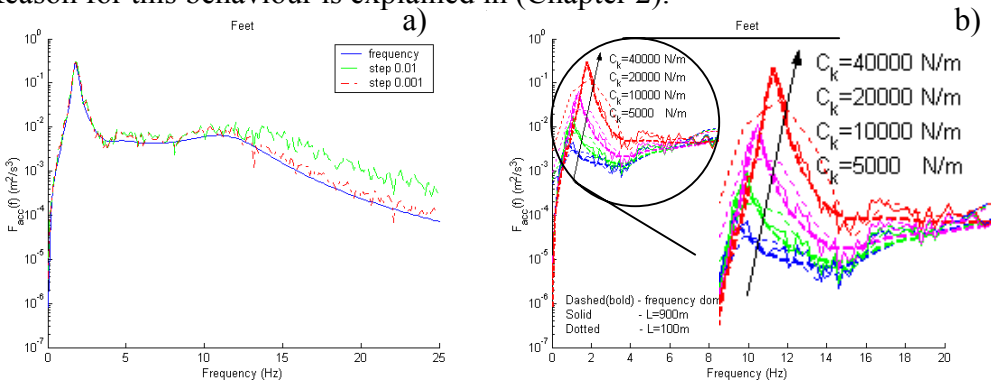

Figure 4: Power spectral density of the chassis acceleration solved **a)** in frequency domain and **b)** through numeric integration with different step sizes and with different traveled length as a function of the carrying spring stiffness C_k.

5 Comparison of the human comfort perception evaluating methods

In the vehicle engineering praxis, optimization of the ride comfort of the car is of interest. The absolute value of the comfort perception is not of big importance in the concept phase, supposed the value is not „too high“.

The carrying spring and the damper are the most common parts to optimize the handling and comfort criteria of a car.

In the following examples we will use the linear quarter car model as described earlier. The car velocity is 20m/s. For the road we have chosen w=2, $G_{uu}(\Omega_{x0}) = 4cm^3$, L=900m, $\Delta\Omega = .01m^{-1}$ for the numerical integration. Our design variables are Ck=[5100, 10000, 20200, 44000] N/m and Dk=[100 500 1140 3000] Ns/m as in [10].

In Figure 5 a) the comparison of the VDI, Klinger and Cucuz perception quantity is showed. The results are calculated in the frequency domain. One can see differencies of 2% in the domain of high stiffness and damping to 6% in the domain of low stiffness and damping for VDI and Cucuz, while the difference between the Cucuz and Klinger criteria is for the whole area very small 0.5 to 1%. The gradients of the surface are nearly the same, which is important for the optimization.

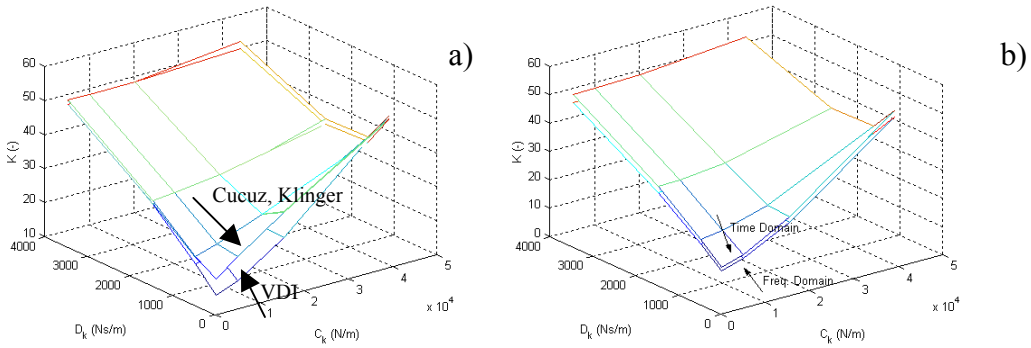

Figure 5: Human comfort perception quantity surface for a carrying stiffness and damper variation. **a)** Comparison of VDI, Klinger and Cucuz criteria in frequency domain **b)** Comparison of the perception quantity after VDI for the frequency and time domain analysis

The results of the numerical integration (time domain) and the frequency analysis are compared in Figure 5 b). The perception quantity resulting from the time domain analysis is about 2.5 (5%) point higher for the domain at higher stiffness and damping and about 1 point (10%) higher for the domain of the low stiffness and damping. Again the gradients of the design surface are again nearly the same.

6 Significance of the non-linearities to the ride comfort optimization

As mentioned before, it is not our intention to predict the absolute value of the comfort perception quantity, but to find the best setup of the vehicle (in terms of carrying spring and damper) under the given external circumstances. Let us now study the influence of the main non-linearities in our car-model (Chapter 4.2).

6.1 Stick-Slip efects in the damper

Because of the assembly of the damper, small coulomb friction is always active. In Figure 6 a) the comparison of the linear model and the non-linear model is shown. We used only the coulomb friction of 10N, which is a quite common value. All other components are linear. The difference of the design surface is very small (about 10%) for low stiffness and damping of the carrying spring and damper. The difference deceases when the stiffness of the carrying spring and damping grows. This is because of the stronger forces acting in the main spring and damper, which dominate against the small coulomb friction. In Figure 6 b) the influence of a bigger coulomb friction forces is pictured. In this case the coulomb friction is significantly stiffening the connection of the unsprung mass to the chassis. This is also the reason why the stiffness of the carrying spring becomes less important with the increasing coulomb friction. The damping amplifies this effect.

Small coulomb friction does not have an important influence to the ride comfort optimization of the vehicle. In opposite, high values of coulomb friction does not enable to make significant changes to the comfort perception quantity using the carrying spring.

6.2 Bump stops

As described earlier, we model the bump stops of the carrying spring with a cubic equation. For large relative displacement amplitudes of the unsprung mass to the chassis

the stiffness rises significantly. Hence the ride comfort is getting worse (Figure 7 a)). For higher damping the relative displacement gets smaller, hence the bump stop is not involved (Figure 7 b)). The bump stop is mostly in action for rough roads. In this section we used w=2, $G_{uu}(\Omega_{x0})$ =64cm^3 and L=900m, $\Delta\Omega$=.01m^{-1} for the road for the numerical integration.

Again, the influence of the non-linearities to the characteristics of the perception surface is not significant for an optimization.

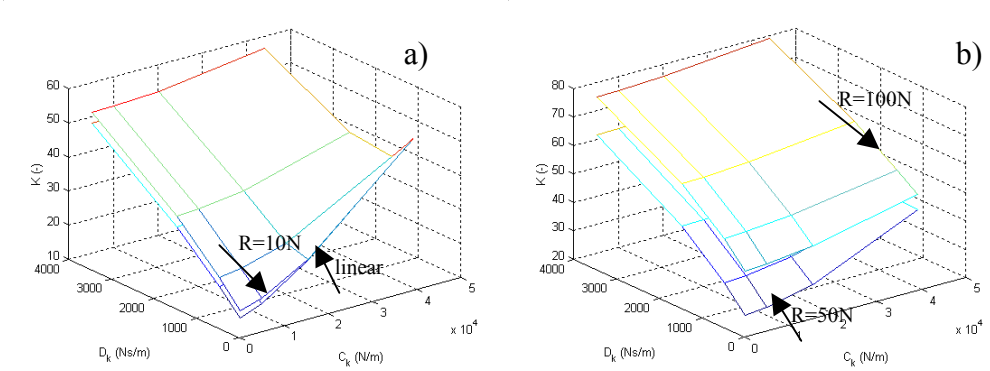

Figure 6: Comparison of the influence of the small coulomb friction on the perception quantity, **a)** linear and R=10N, **b)** R=50N and 100N

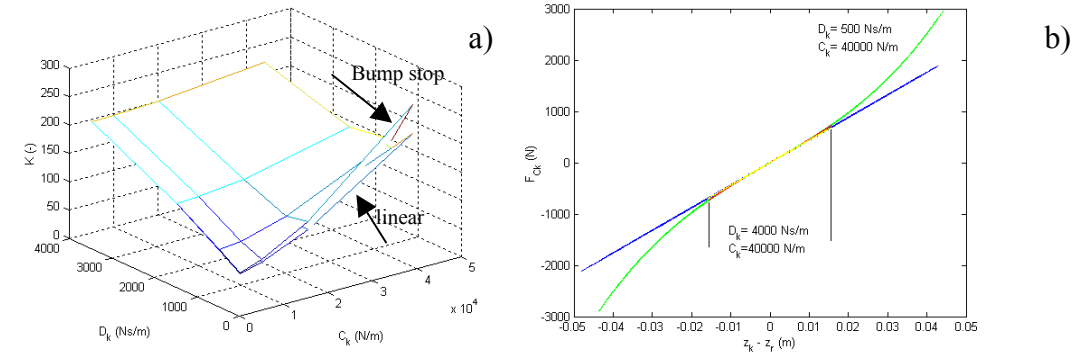

Figure 7: **a)** Comparison of the influence of a bump stop to the perception quantity for a rough road (w=2, $G_{uu}(\Omega_{x0})$ =64cm^3). **b)** The force of the carrying spring with a bump stop for different damping D_k, note the different displacement bias.

6.3 Non-linear Damper

The non-linear damper is represented by a non-linear Maxwell element using a cubic equation for the inverse damper characteristics. We chose a common non-linear damper characteristic. To be able to make a comparison with the preceding models we scaled the characteristic in a way, that the linear interpolation is the same as the former linear damping (Section 5). Figure 8 shows the comparison for a federal road a) and for a rough road b). The difference between the linear and the non-linear model is now more visible (between –20% to 20%).

6.4 Summary of the significance of non-linear modeling to the objective function

Let us now act all three cases at once. Again we will use the federal road (w=2, $G_{uu}(\Omega_{x0})$ =4cm^3, L=900m, $\Delta\Omega$=.01m^{-1}) and the rough road (w=2, $G_{uu}(\Omega_{x0})$ =64cm^3, L=900m, $\Delta\Omega$=.01m^{-1}). Our objective function is the sum of the normalized human

perception quantity and normalized distribution of the normal tire force. In Figure 9 the surface of the objective for the federal road a) as well the gradients b) of the surface are plotted. The same results are pictured in Figure 9 for a rough road c) and d). The gradients of the two surfaces are similar. The reason for the better coincidence of the results of the rough road is the linearization of the damper characteristics, which was done for the whole characteristics. For the rough road this condition is fulfilled better. For small friction the results are comparable with the results where only linear car-model was used. For greater friction (50N) the objective function is distorted and the optimum would be found for less damping.

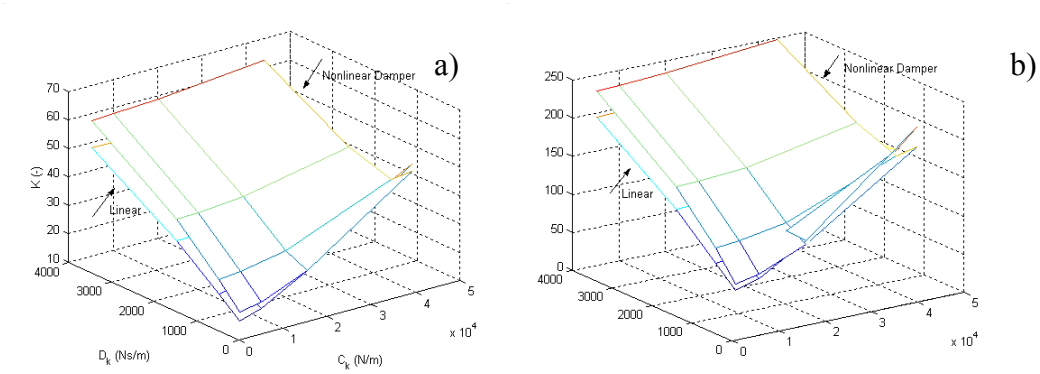

Figure 8: Comparison of the influence of a non-linear damping to the perception quantity for **a)** a federal road (w=2, $G_{uu}(\Omega_{x0})$ =4cm^3) and **b)** a rough road (w=2, $G_{uu}(\Omega_{x0})$ =64cm^3).

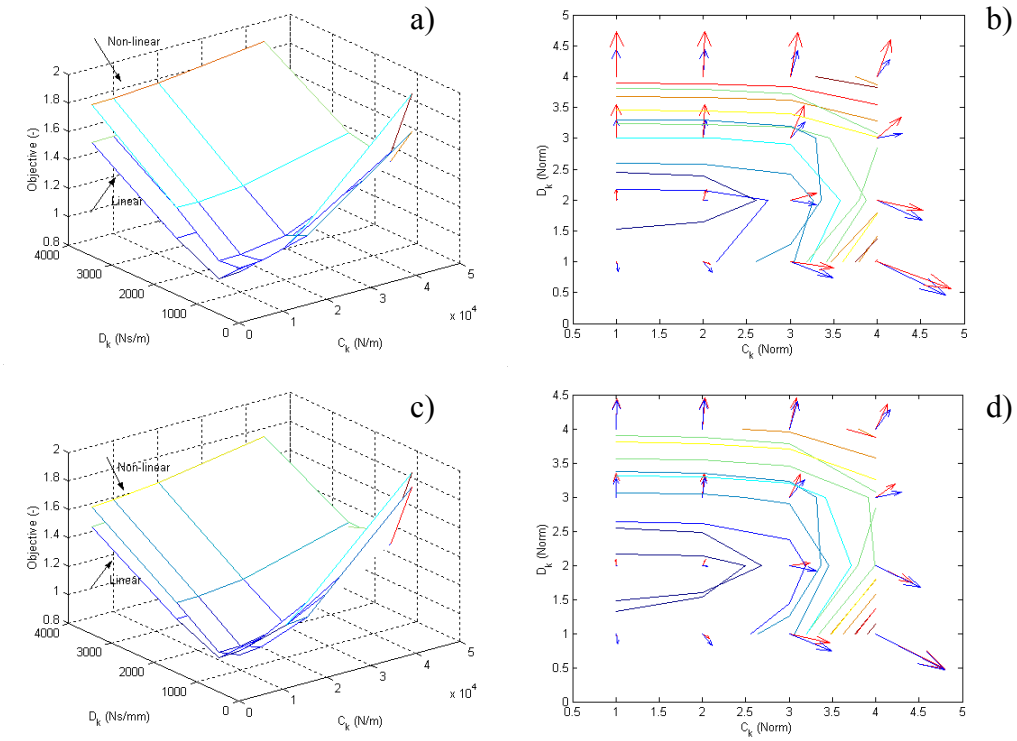

Figure 9: Comparison of the influence of the non-linear elements to the ride comfort objective for a variation of the carrying stiffness and scaled non-linear damping. **a)** Federal road (w=2, $G_{uu}(\Omega_{x0})$ =4cm^3) **b)** the according gradients of the objective surface (red non-linear, blue linear) **c)** rough road (w=2, $G_{uu}(\Omega_{x0})$ =64cm^3) **d)** the according gradients of the objective surface (red non-linear, blue linear)

7 Summary

In the paper the influence of the components non-linearities on the optimization of the ride comfort of a quarter car model was studied. The results of a numerical integration for a linear model were validated with the results of a frequency domain solution. Considered the Nyquist rule for the sampling theorem for the integration as well as for the road generation the results are suitable for further investigations. Several methods for evaluating the human comfort perception quantity were cited. They are different in evaluation of the absolute value of the perception quantity, but are very well comparable for the optimization of the ride comfort. We then introduced main non-linear properties of the vertical car dynamics to the linear model. Modifications of the non-linear parameters were so applied, that the linearized model was comparable with the already introduced linear model. A sum of the normalized human perception quantity and the normalized normal tire force distribution was used as the objective function. For a medium non-linear behavior, which can be supposed for ride comfort on civil roads, the qualitative characteristics of the optimization surface are comparable with the corresponding characteristics of the linear model.

8 Acknowledgment

This research was supported, in part, by the Grant Agency VEGA No. 1/9432/02.

9 References

[1] Parchilovksij, J. G.: Spektrale Verteilungsdichte der Unebenheiten des Mikroprofils der Strassen und die Schwingungen des Kraftfahzeugs. Automobilnaja Promišelnost XXVII Jahr, Nr. 10 1961.

[2] Silajev A. A.: Spektralnaja teoria podressorivania transportnych mašin Mašinostrojenie Moskva 1972.

[3] Braun,H.: Untersuchungen von Fahrbahnunebenheiten und Anwendung der Ergebnisse Dissertation TU Braunschweig 1969.

[4] VDI2057 Blatt 1: Einwirkung mechanischer Schwingungen auf den Menschen. Grundlagen, Begriffe 1987.

[5] VDI2057 Blatt 2: Einwirkung mechanischer Schwingungen auf den Menschen. Bewertung 1987.

[6] VDI2057 Blatt 3: Einwirkung mechanischer Schwingungen auf den Menschen. Beurteilung 1987.

[7] ISO 5982: Vibration and shock – Mechanical driving point impedance of the human body 1981.

[8] Cucuz S.: Schwingempfindung von Pkw-Insassen. Auswirkungen von stochastischen Unebenheiten und Einzelhindernissen der realen Fahrbahn. Dissertation der Fakultät für Maschinenbau und Elektrotechnik der TU Braunschweig, 1992.

[9] Klinger B.: Einfluß der Motorlagerung auf Schwingungskomfort und Geräuschanregungen im Kraftfahrzeug. Dissertation, TU Braunschweig, 1996.

[10] Mitschke, M.: Dynamik der Kraftfahrzeuge, Band B Schwingungen 2. Auflage Springer Verlag, Berlin Heidelberg New York Tokyo 1984.

[11] Richter, B.: Schwerpunkte der Fahrzeugdynamik: Fahrzeugschwingungen, Kurshaltung, Vierradlenkung, Allradantrieb Verl. TÜV Rheinland, 1990.

[12] Kolsch H.: Schwingungsdämpfung durch statische Hysterese VDI, 1993.